Journal of Chemical Health Risks

www.jchr.org

JCHR (2024) 14(1), 629-646 | ISSN:2251-6727

Efficacy of Resveratrol and Cisplatin on Biological Activities of Human Tongue Squamous Cell Carcinoma Cell Lines

Maged Ali Ali Muthanna[1], Sanaa Mahmoud Anis Saleh[2], Heba E.M. Youssef[3].
1,2,3 Department of Oral and Maxillofacial pathology, Faculty of Dentistry, Tanta University, Egypt.

(Received: 27 October 2023 Revised: 22 November Accepted: 26 December)

KEYWORDS

Tongue squamous cell carcinoma, Cell Lines, Resveratrol, Cisplatin, Cell viability, Cell migration, Epithelial mesenchymal transition.

ABSTRACT:

Background: Chemotherapeutic agents as cisplatin (Cis) often showed drug resistance, and various side effects. Thus, the development of novel therapeutic approaches is needed. Resveratrol (RSV) is a natural phytochemical agent with anticarcinogenic activities.

Aim of the study: This study was conducted to investigate the efficacy of RSV with or without different doses of Cis on the biological activities of human tongue squamous cell carcinoma (TSCC) cell lines; namely the viability, migration, and epithelial-mesenchymal transition (EMT) of such tumor cells.

Material and Methods: TSCC cell lines (CAL-27) were used and classified into 6 groups. Intervention agents of RSV with or without Cis at different concentrations were applied. MTT assay and wound healing assay were used to analyze the inhibition of cell proliferation (viability) and the migration of cancer cells, respectively. EMT was investigated by assessment of the immunocytochemical Slug expression.

Results: MTT assay demonstrated that application of RSV or Cis separately inhibited cell viability in a concentration-dependent manner. The combination treatment of RSV and Cis had more cytotoxic effects against cancer cells. Moreover, wound healing assay showed that the combination of RSV with Cis had synergistic inhibition effect on cancer cell migration more than that of single agent treatment. Immunocytochemical assessment showed that combination of RSV with Cis inhibits EMT through reducing Slug expression.

Conclusion: The combination of RSV with Cis could be used as a promising approach for OSCC therapy as they reduced cancer cell viability, migration and inhibited EMT with minimal side effects.

1. Introduction

Globally, it is nearly about one million persons are affected annually by head and neck cancers (HNCs), it is the sixth most prevalent malignant tumor [1]. Oral squamous cell carcinoma (OSCC) is one of the most frequent malignancies of the HNCs [2]. Regardless of the application of novel therapeutic modalities in the latter decade, the 5-year global survival rate of OSCC presently does not exceed 55% [3]. According to the data given by the World Health Organization (WHO) in 2020, oral cancer caused 544 deaths in Egypt, or 0.61 percent of all fatalities [4].

Cisplatin (Cis), a chemotherapeutic drug, has a potent antitumor effect against a wide variety of malignancies. In clinical applications, it is the first-line and most commonly employed treatment for OSCC [5]. Unfortunately, with the increased usage of Cis in recent years, many patients have encountered hazardous side effects [6]. Therefore, there is extremely attention on alternative treatments to discover new, safe, and effective agents against cancer. Resveratrol is a natural non-flavonoid polyphenol compound. It consists of two phenolic rings attached by a styrene double bond to generate 3,4,5-trihydroxystilbene, which appears in trans- and cis-isoforms (Fig. 1). The trans-isoform is the

Journal of Chemical Health Risks

www.jchr.org

JCHR (2024) 14(1), 629-646 | ISSN:2251-6727

general isoform and represents the most extensively researched chemical form [7].

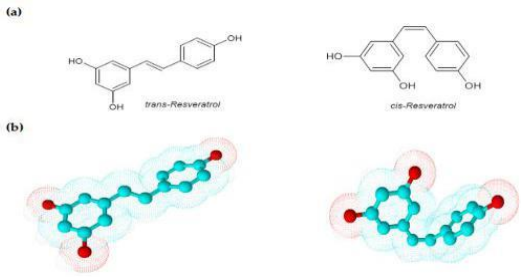

Fig. (1): (a) Chemical structures of trans-RSV and cis-RSV; (b) 3D chemical structures of trans-RSV and cis-RSV; cited from **Berretta et al., (2020)** [8].

Epithelial-mesenchymal transition (EMT) is characterized by a dynamic change in cellular architecture from epithelial to mesenchymal phenotypes, which induces biological behavioral changes in cells leading to migration and invasion [9]. EMT state has been correlated to aggressiveness and poor prognosis in OSCC. Molecular biological markers have been proposed as useful for detecting EMT. The overexpression of EMT-transcription factors (EMT-TFs) such as Slug display a significant association with poor overall survival among OSCC patients. These biomarkers might improve the capacity to estimate the biological development of OSCC [10]. Still, not much is known about the action of RSV in conjunction with different doses of Cis in treatment of human TSCC which requires further investigation.

This study was conducted to investigate the efficacy of RSV with or without different doses of Cis on the biological activities of human tongue squamous cell carcinoma (TSCC) cell lines; namely the viability, migration, and epithelial-mesenchymal transition (EMT) of such tumor cells.

2. Material and Methods

2.1 Materials

All the steps of the current experiment were taken place in Confirmatory Diagnostic Unit, Veterinary Serum & Vaccine Research Institute, Cairo, Egypt (51 Wezaret Al Zeraa Street, Dokki, Giza – Egypt). (VACSERA-Egypt). Human tongue carcinoma cell line (CAL-27) was purchased from VACSERA. It was brought from the "American Type culture Collection" (ATCC), stored in liquid nitrogen containers at -196 C°. Resveratrol (RSV) was purchased from Sigma-Aldrich Company (43 Nazeeh Khalifa Street. Heliopolis, Cairo, Egypt). Cisplatin (Cis) and Ready for use anti Slug antibody (mouse monoclonal antibody) vial of 5 ml were purchased from Dako Company (9 Al-Obour, Salah Salem Road. Heliopolis, Cairo – Egypt).

2.2. Methods

2.2.1. Preparation of Interventions

RSV was dissolved in DMSO to prepare different concentrations (5, 10, 20, 50 and 100 µg/ml) needed for the experiment [11]. Cis was dissolved in distilled water to prepare different concentrations (0.625, 1.25, 2, 5, 10 µg/ml) needed for the experiment [1213]. Anti Slug antibody was ready for use, at concentration (1:100) [14].

2.2.2. Culture of CAL-27

Cell lines were cultured with Dulbecco's modified Eagle's medium (DMEM), 10% FBS and 2% Streptomycin-Penicillin. CAL-27 was sub-cultured to obtain 6 groups and classified them as illustrated in table (1).

Table (1): The study design.

Group	Details
A	Control
EXR	Experimental subgroup that was treated with IC50 of RSV for 48 hours
EXC2	Experimental subgroup that was treated with Cis 2 µg/ml for 48 hours
EXC5	Experimental subgroup that was treated with Cis 5 µg/ml for 48 hours
EXR/C2	Experimental subgroup that was treated with IC50 of RSV and Cis 2 µg/ml for 48 hours
EXR/C5	Experimental subgroup that was treated with IC50 of RSV and Cis 5 µg/ml for 48 hours

Journal of Chemical Health Risks

www.jchr.org

JCHR (2024) 14(1), 629-646 | ISSN:2251-6727

2.2.3. MTT assay

IC50 Value Calculation and experiment

CAL-27 cells were initially seeded at a density of 1 X 10^4 cells per well in a 96-well culture plate and then incubated for 24 hours within a 5% CO2 incubator before conducting the MTT assay. Subsequently, the wells of the culture plate were subjected to distinct concentrations of RSV (5, 10, 20, 50, and 100 µg/ml) and separate concentrations of Cis (0.625, 1.25, 2, 5, and 10 µg/ml). In parallel, the control group underwent treatment with DMSO. The determination of IC50 values for both RSV and Cis involved calculating the concentration at which 50% cell growth inhibition occurred following a 48-hour exposure to the respective drugs, in comparison to untreated control cells.

The culture plate wells were initially treated with a combination of IC50 of RSV (Resveratrol) with 2 µg/ml of Cisplatin and IC50 of RSV with 5 µg/ml of Cisplatin. This treatment was followed by a 48-hour incubation period in a CO2 incubator. Subsequently, the culture plate was processed as follows: the culture medium was removed, and the cells were then incubated with medium containing 0.5 mg/ml MTT for a duration of 4 hours at 37 °C in a 5% CO2 atmosphere. Following this incubation, the medium was aspirated, and the formazan product formed was solubilized using DMSO. The optical density of the purple formazan crystals dissolved in isopropanol in each well was then spectrophotometrically measured at a wavelength of 450 nm using an ELISA microplate reader. It is noteworthy that all experiments were conducted in triplicate to ensure robustness and reliability of the results.

2.2.4. Wound Healing Assay

CAL-27 cells were initially seeded in a 24-well plate at a density of (1 X 10^4) cells per well, utilizing wound healing dish inserts. Following incubation in the cell culture incubator for 24 hours, a monolayer was established. Subsequently, the cells underwent a PBS wash, after which they were incubated with FBS-free culture medium to eliminate potential influences of FBS on cell migration. The inserts, creating a scratch with a width of 0.9 mm, were then removed from the wells. The cell cultures were subjected to treatment with the IC50 of RSV and Cis, in accordance with the experimental groups outlined in the current protocol. Capturing images of the scratches occurred at three distinct time points: 0, 24, and 48 hours, utilizing an inverted microscope. To assess the wound width, Olympus Cell Sens Dimension software was employed for the analysis. This entire assay was conducted in triplicate to ensure robustness and reliability of the results [15].

2.2.5. Immunocytochemical (ICC) Staining of Slug for EMT Analysis

In accordance with the current protocol, a 150 cm^2 flask containing 1x 10^8 cells per flask for all groups underwent centrifugation at 3000 rotations per minute (rpm) for 5 minutes at room temperature. This process aimed to harvest cell pellets, except for the EXR/C5 group, where a cell pellet could not be obtained due to the extremely low number of viable cells. Subsequently, the obtained pellet was washed and suspended in 2ml of PBS, followed by centrifugation for an additional 5 minutes at 3000 rpm. The resulting pellet was then suspended in 10% formalin at room temperature for a duration of 1 hour. Following formalin fixation, the suspension underwent centrifugation at 1500 rpm for 5 minutes. Using a sterile wooden applicator stick, care was taken to delicately extract the cell pellets from the tube, transferring them into appropriately labeled cassettes. The next step involved the dehydration of the cell pellets in various ethanol concentrations (50, 70, 95, and 100%). Subsequently, the labeled cassettes were immersed in xylene baths for 2 minutes before being embedded in paraffin blocks. This embedding process was crucial for obtaining 4-µm sections [16,17]. Paraffin blocks of, A, EXR, EXC2, EXC5, and EXR/C2 groups were sliced into 4-micron thick sections and placed on positively charged (OptiPlus) slides for staining procedures [18].

2.2.6. Statistical Analysis

All group data were statistically analyzed with Statistical Package for the Social Sciences (SPSS) (version 19, IL, USA) was used. One way ANOVA followed by multiple comparison Tukey's test were performed to detect significance between groups.

3. Results

3.1.MTT Assay

3.1.1. Effects of RSV

After 48 hours of MTT testing of CAL-27 cell lines, over the pre-determined dose range of RSV (5, 10, 20, 50, 100 µg/ml), the cytotoxic activity of RSV was assessed. The percentage of cell viability showed gradual decrease with increasing concentration of RSV as shown in Fig. (2). The IC50 value was 28.45 µg/ml, calculated from a graph of cell viability obtained over a range of those doses. Mean and standard deviation (SD)

Journal of Chemical Health Risks

www.jchr.org

JCHR (2024) 14(1), 629-646 | ISSN:2251-6727

values of viability of CAL-27 cell lines show a highly significant difference between subgroups with P ≤ 0.001.

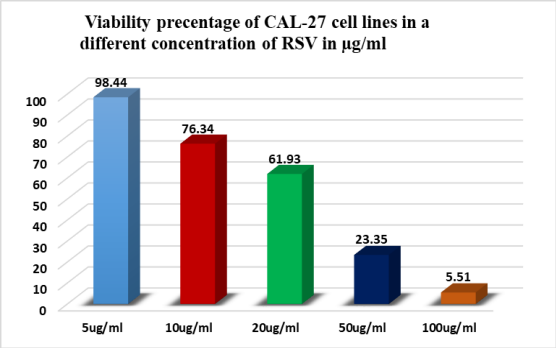

Fig. (2): Bar chart diagram showing cell viability percentage of cancer cells at different concentrations of RSV.

3.1.2. **Effects of Cis:**

Likewise, the cell viability percentage showed gradual decrease with increasing concentrations of Cis (0.625 µg/ml, 1.25 µg/ml, 2 µg/ml, 5 µg/ml, 10 µg/ml) as shown in Fig. (3). The IC50 value was 1.93 µg/ml, Mean and SD values show a highly significant difference between subgroups with P ≤ 0.001.

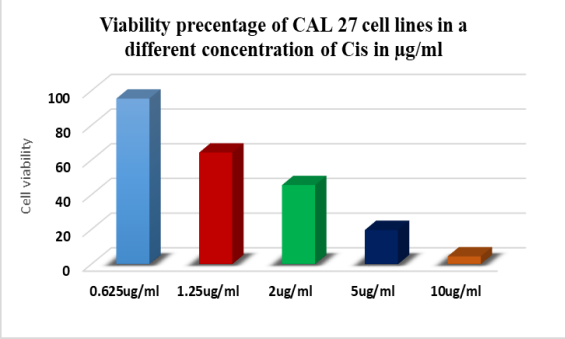

Fig. (3): Bar chart diagram showing cell viability percentage of cancer cells at different concentration of Cis.

3.1.3. **Effects of RSV with Cis**

In EXR/C2 and EXR/C5 groups the cell viability percentage was 15% and 3%, respectively. These results were the lowest cell viability in comparison to the control group or to single-treated groups as shown in Fig. (4). Mean and SD values of viability of CAL-27 cell lines in control and experimental groups were exhibited a highly significantly different values between them according to multiple comparison Tukey's test (P ≤ 0.001).

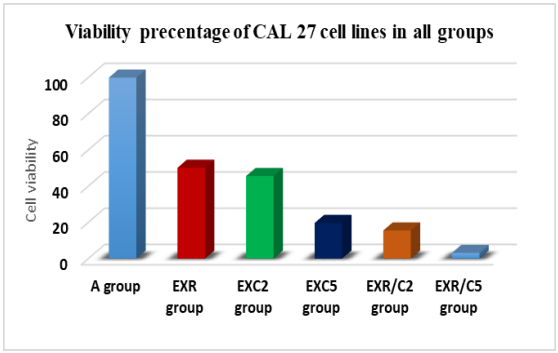

Fig. (4): Bar chart diagram showing cell viability percentage of cancer cells in control and experimental groups.

3.2. **Morphological Assessment**

Morphological changes of cell line CAL-27 were observed and assessed using the inverted phase contrast microscope (X100) by recording the change in the state of cell line in control group as well as the experimental groups (Figs 5-10). In the control group, the epithelial cells showed their typical polygonal shape with definite outline and central nuclei. The cell lines demonstrated attachment and confluency throughout microscopic field (Fig. 5). In EXR group, cytotoxic effect was observed by reduction of cell number and exhibited some morphological changes than that in control group as loss of attachment and cellular aggregation. (Fig. 6 A, B). In EXC2 group, more loss of cellular attachment and confluency were noted than EXR group. Cis showed potent growth inhibitory effect on cultured cells than RSV revealed by more reduction of cell number in EXC2 group than in EXR group (Fig. 7 A, B). In EXC5 group, decreased cancer cell growth was greater revealed by more reduction in cell number and increased cellular morphological changes with more appearance of apoptotic cells and pyknotic nuclei (Fig. 8 A, B). The cellular morphological changes and growth inhibition features became more prominent in combination experimental groups (EXR/C2 and EXR/C5) (Fig. 9 A, B and Fig. 10 A, B), respectively, compared to the single-drug groups (EXR, EXC2 and EXC5) with marked decrease in cell viability and increased morphological changes)

Journal of Chemical Health Risks

www.jchr.org

JCHR (2024) 14(1), 629-646 | ISSN:2251-6727

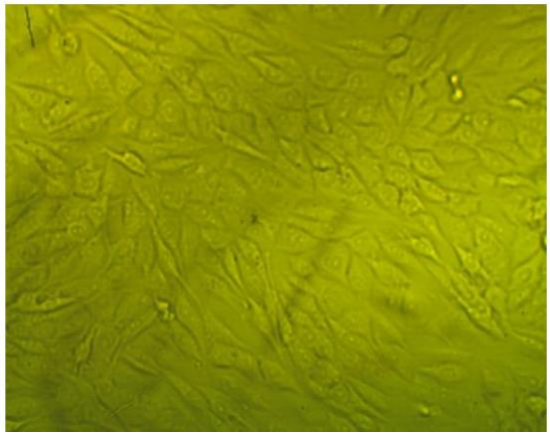

Fig. (5): A photomicrograph shows cell viability of CAL-27 in control group showing confluency with adherent cells and central nuclei. Typical polygonal cell morphology is observed. (Inverted phase contrast microscope filter X100)

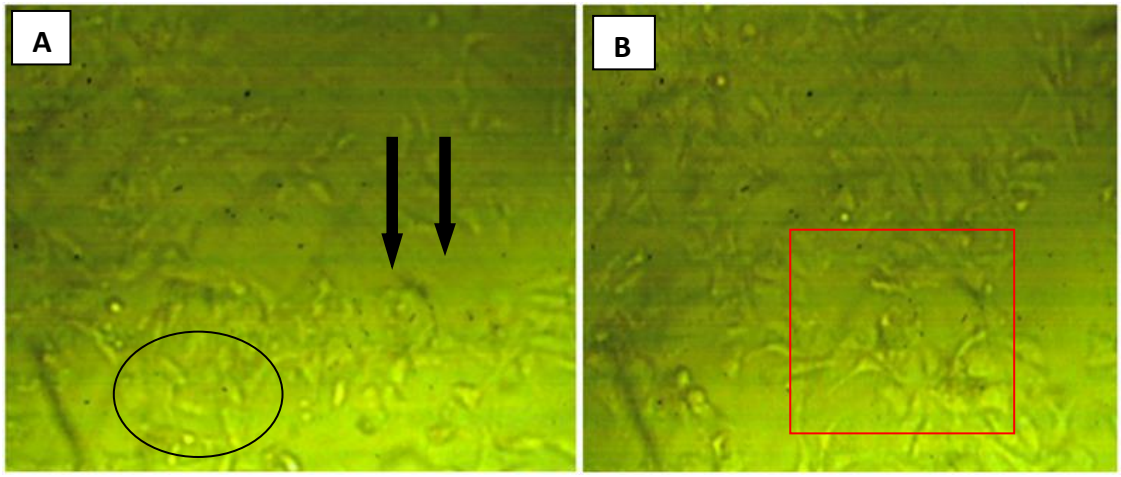

Fig. (6): Photomicrographs showing cell viability of cancer cells in EXR group. (A) Complete loss of cells (Black arrows), loss of attachment (Black circle). (B) Cellular aggregation and blurred cell outline (Red square). (Inverted phase contrast microscope filter X100)

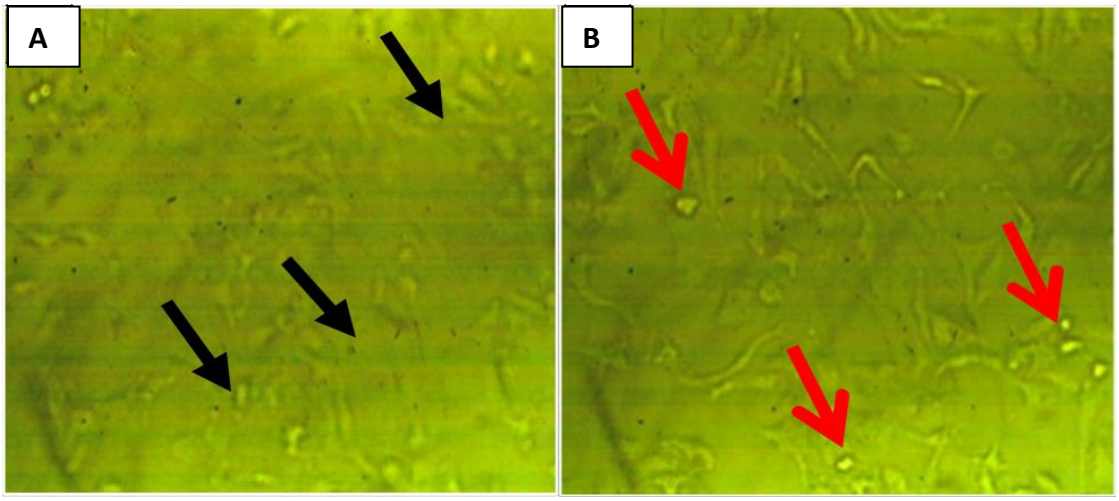

Fig. (7): Photomicrographs showing cell viability of cancer cells in EXC2 group. (A) Complete loss of cells (Black arrows). (B) Apoptotic cells with blebbing (Red arrows) (Inverted phase Contrast Microscope filter X100)

Journal of Chemical Health Risks

www.jchr.org

JCHR (2024) 14(1), 629-646 | ISSN:2251-6727

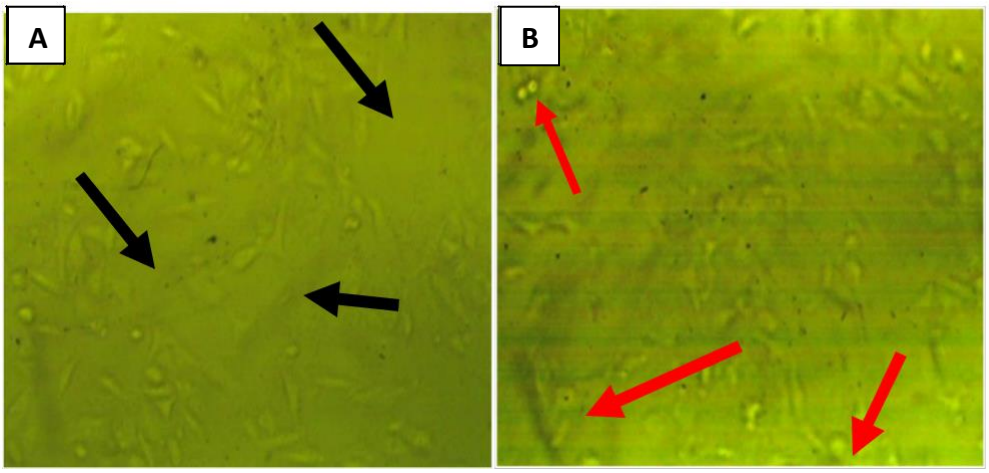

Fig. (8): Photomicrographs showing cell viability of cancer cells in EXC5 group. (A) Complete loss of cells **(**Black arrows). (B) Apoptotic cells (Red arrows). (Inverted phase contrast microscope filter X100)

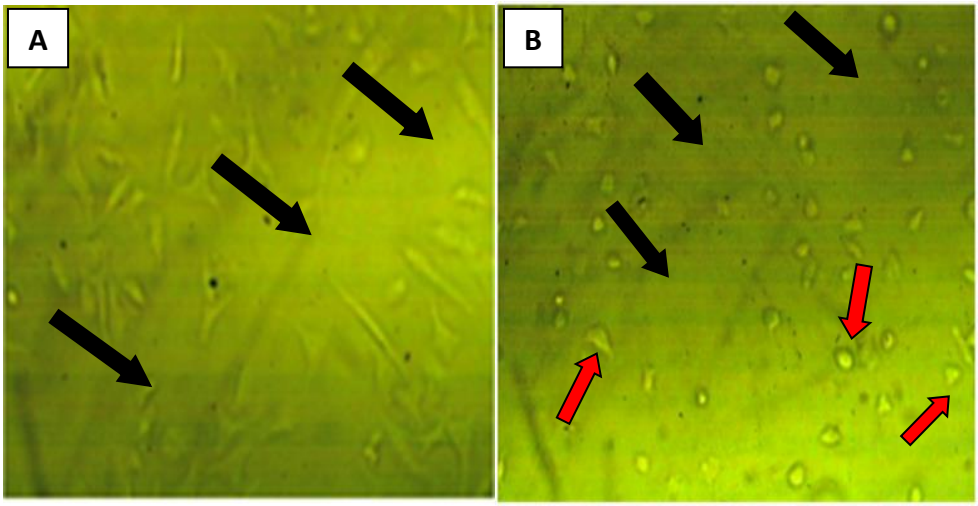

Fig. (9): Photomicrographs showing cell viability of cancer cells in EXR/C2 group. (A & B) Marked loss of cells **(**Black arrows), numerous apoptotic cells with blebbing are observed (Red arrows). (Inverted phase contrast microscope filter X100)

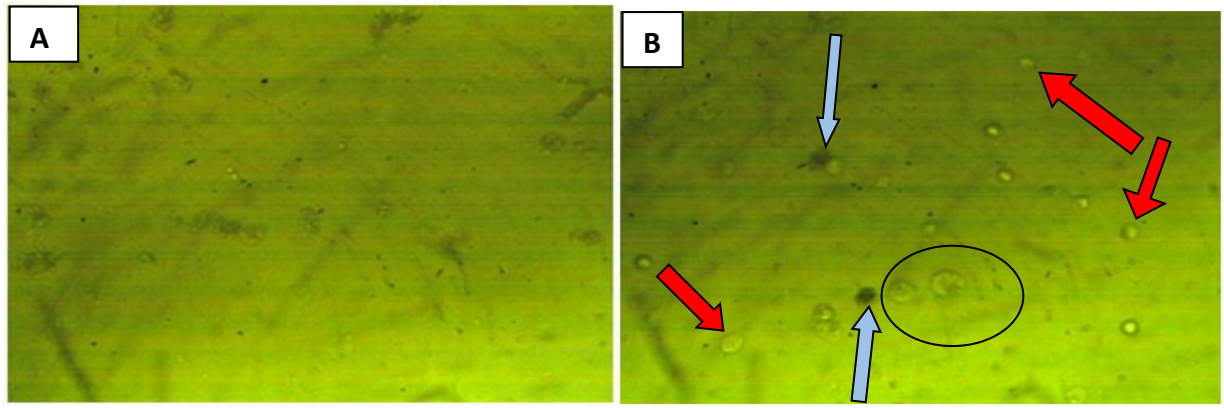

Fig. (10): Photomicrographs showing cell viability of cancer cells in EXR/C5 group. (A) Marked loss of cells (B), numerous apoptotic cells (Red arrows), chromatin clumping (Blue arrows), cellular swelling (Black circle) (Inverted phase contrast microscope filter X100)

Journal of Chemical Health Risks

www.jchr.org

JCHR (2024) 14(1), 629-646 | ISSN:2251-6727

3.3. Effects of RSV and Cis alone or in combination on migration

In wound healing assay the average wound healing closure percentage at 48 h was gradually decreased from; 54.8% for EXR group, 45.7% for EXC2 group, 32.4% for EXC5 group, 22.6% for EXR/C2group and 12.4% for EXR/C5 group, while the wound width ratio of untreated group was 93.3%. In comparison with control group, the migration of the treated cells was inhibited. RSV as well as Cis reduced the migration capability of CAL-27 cell lines. The migration of CAL-27 cell lines was at lowest value for the combination groups (EXR/C2 and EXR/C5). Thus, RSV with Cis had the highest antimigratory effects of CAL-27 cell lines as shown in Fig. (11).

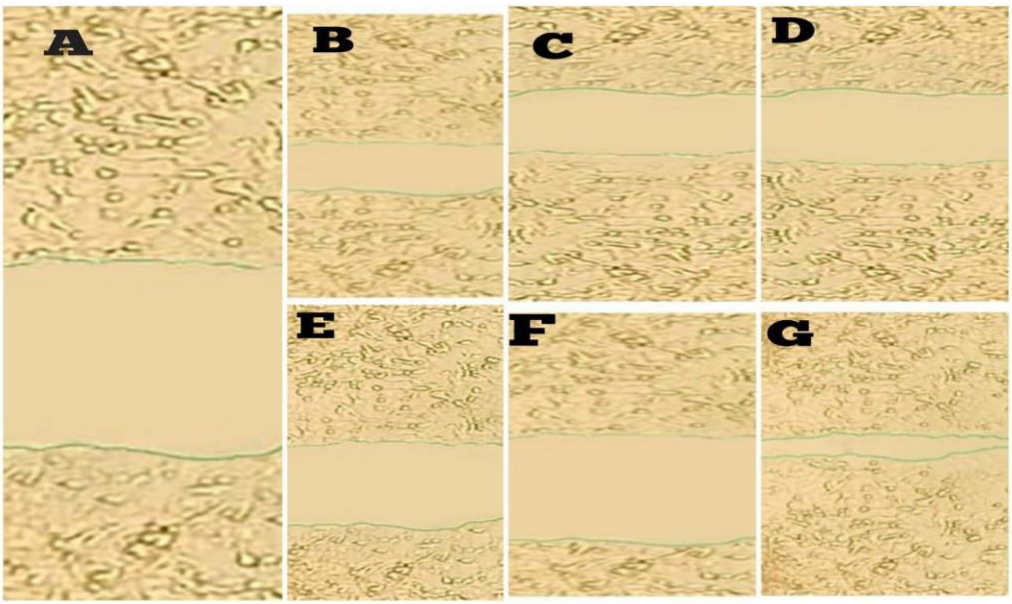

Fig. (11): Photomicrographs showing migration into the wound space photographed at the time of initial wounding and at 48 h after wounding. (A) At the time of scratching, (B) At 48 h, EXR group, (C) At 48 h, EXC2 group, (D) At 48 h, EXC5 group, (E) At 48 h, EXR/C2 group, (F) At 48 h, EXR/C5 group and (G) At 48 h, control group.

Mean and SD values of wound closure (%) for all groups were presented in table (2) and Fig. (12) which show a highly significant difference between groups with $P \leq 0.001$. These studied groups demonstrated a highly significantly different values between them according to multiple comparison Tukey's test $P \leq 0.001$ as revealed in table (3)

Table (2): Mean and SD of wound healing closure percentage of cancer cells in control and experimental groups (One-way ANOVA - test).

Mean and SD of wound healing closure percentage results				
Groups	Mean (%) ± SD	Min--Max	F	P-value
A	93.30±1.01	92.30—94.30	1241.938	0.001**
EXR	54.80±2.01	52.80—56.80		
EXC2	45.70±1.01	44.70—46.70		
EXC5	32.40±1.01	31.40—33.40		
EXR/C2	22.60±1.01	21.60—23.60		
EXR/C5	12.40±2.01	10.40—14.40		

**$P \leq 0.001$ is highly significant

Journal of Chemical Health Risks

www.jchr.org

JCHR (2024) 14(1), 629-646 | ISSN:2251-6727

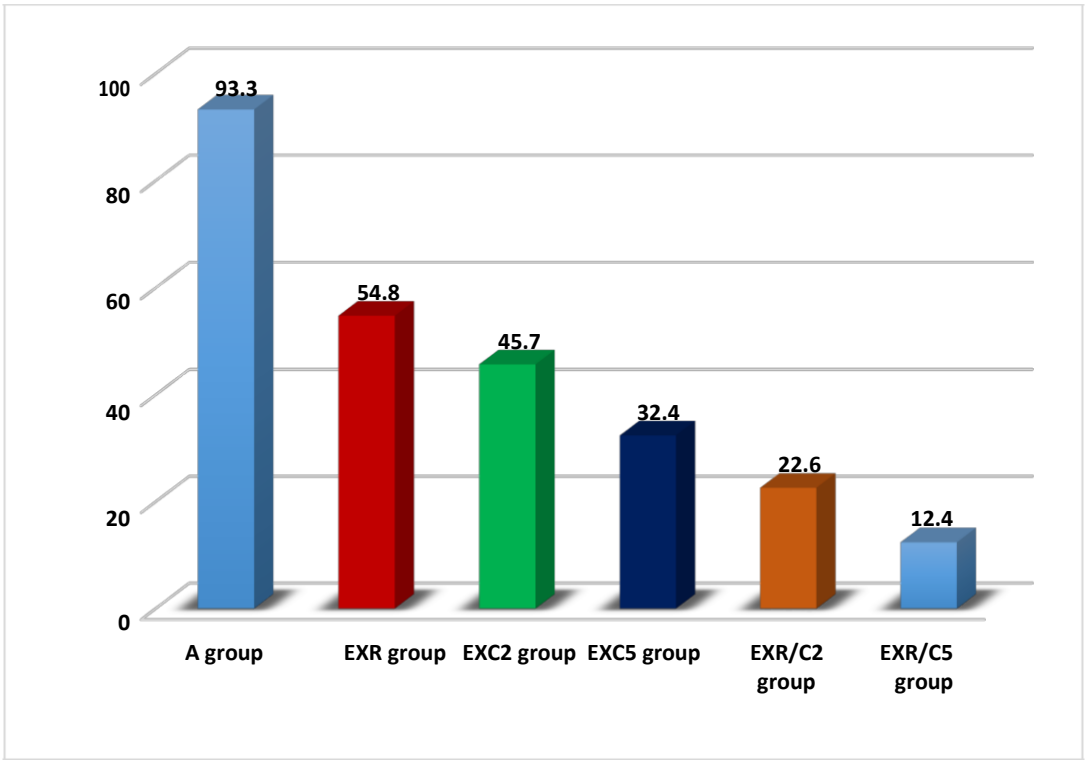

Fig. (12): Bar chart diagram showing wound healing closure percentage of cancer cells in control and experimental groups.

Table (3): Difference between the studied groups measured by Tukey's test in wound healing assay.

Multiple comparison Tukey's test of wound healing						
Groups	A	EXR	EXC2	EXC5	EXR/C2	EXR/C5
A	------	0.001**	0.001**	0.001**	0.001**	0.001**
EXR	0.001**	------	0.001**	0.001**	0.001**	0.001**
EXC2	0.001**	0.001**	------	0.001**	0.001**	0.001**
EXC5	0.001**	0.001**	0.001**	------	0.001**	0.001**
EXR/C2	0.001**	0.001**	0.001**	0.001**	------	0.001**
EXR/C5	0.001**	0.001**	0.001**	0.001**	0.001**	------

**P ≤ 0.001 is highly significant

3.4. Effects of RSV and Cis alone or in combination on EMT

In the negative control specimens, the cells were negative as shown in Fig. (13) as the primary antibody was omitted. ICC expression of Slug exhibited nuclear immunostaining that decreased in comparison with the control group, that showed the highest values, followed by the EXR group, EXC2 group, EXC5 group and finally reached lowest values in the combination group EXR/C2 Fig. (14-18). Due to the high toxicity of RSV when added to 5 µg/ml of Cis, the pellet could not obtained from EXR/C5 group.

Journal of Chemical Health Risks

www.jchr.org

JCHR (2024) 14(1), 629-646 | ISSN:2251-6727

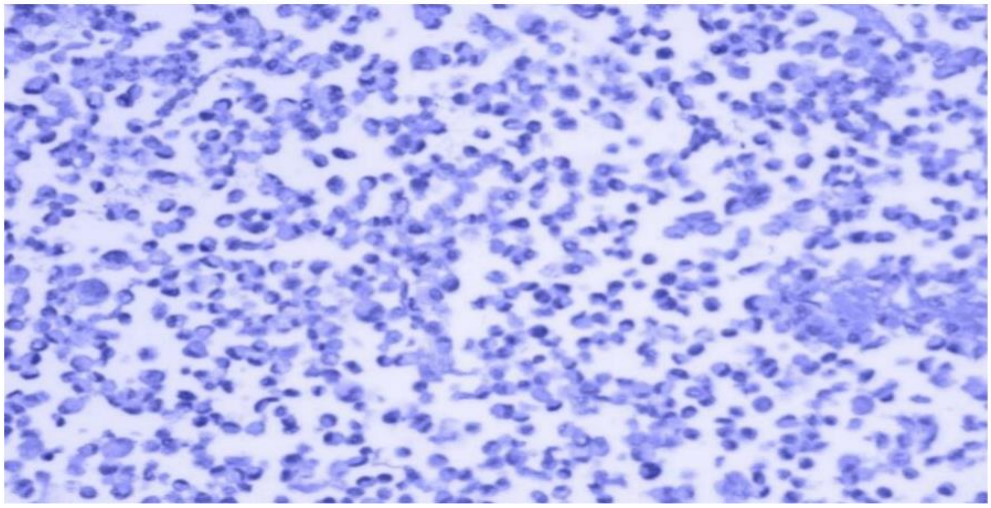

Fig. (13): A photomicrograph of the negative control (without anti-slug antibody) shows negative immunostaining expression (x 100).

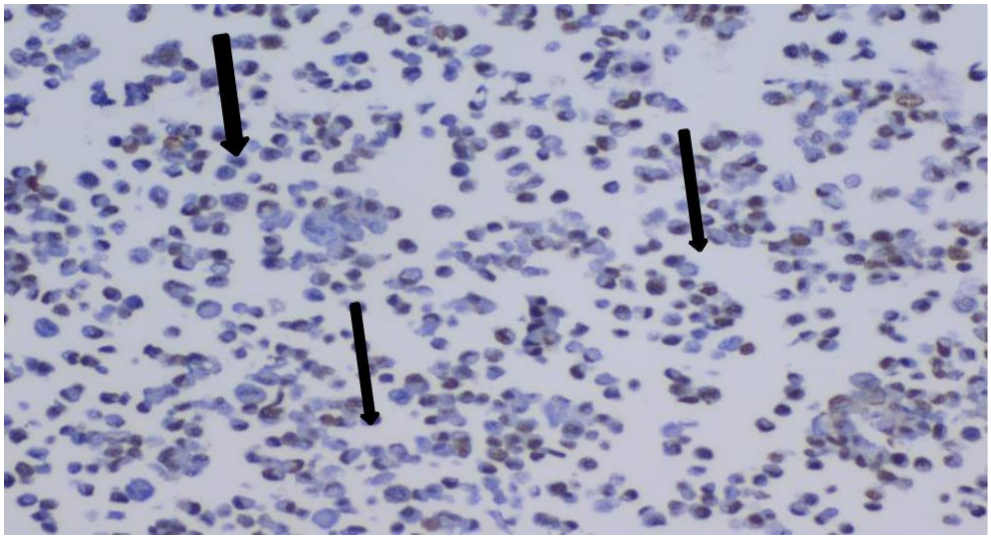

Fig. (14): A Photomicrograph of control group shows strong nuclear Slug immune expression (Black arrows) (ABC x 100)

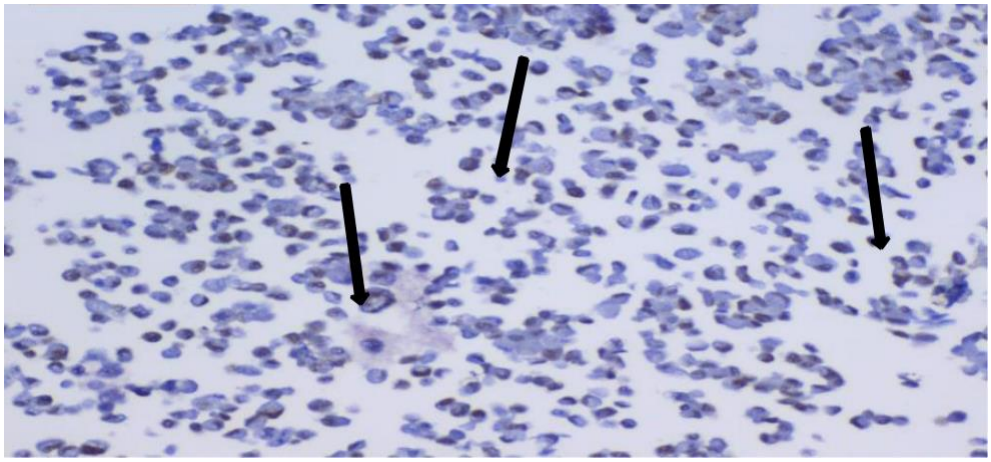

Fig. (15): A Photomicrograph of EXR group shows moderate nuclear Slug immune expression (Black arrows) (ABC x 200).

Journal of Chemical Health Risks

www.jchr.org

JCHR (2024) 14(1), 629-646 | ISSN:2251-6727

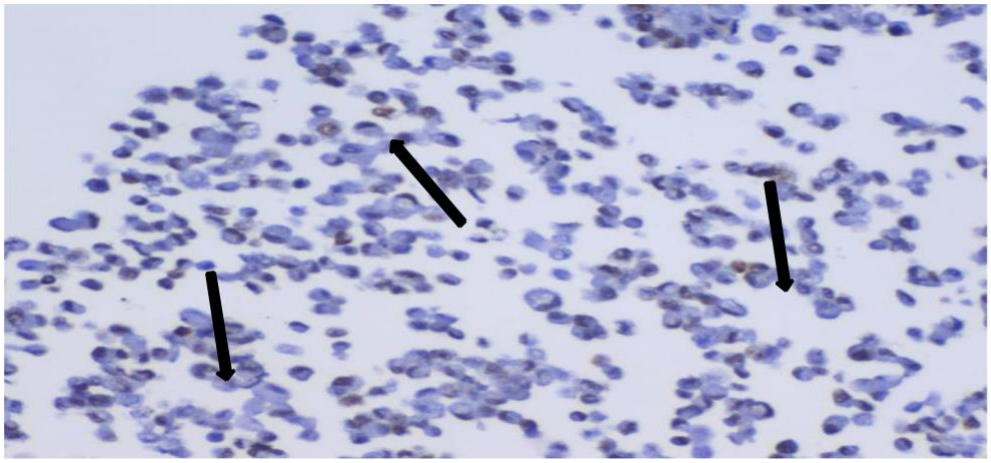

Fig. (16): A Photomicrograph of EXC2 group shows moderate nuclear Slug immune expression. (Black arrows) (ABC x 200).

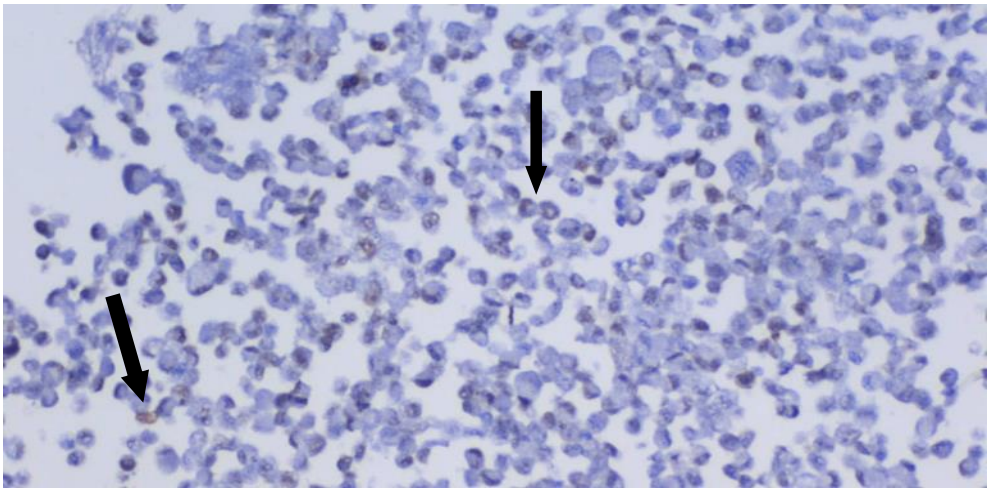

Fig. (17): A Photomicrograph of EXC5 group shows weak nuclear Slug immune expression (Black arrows) (ABC x 100).

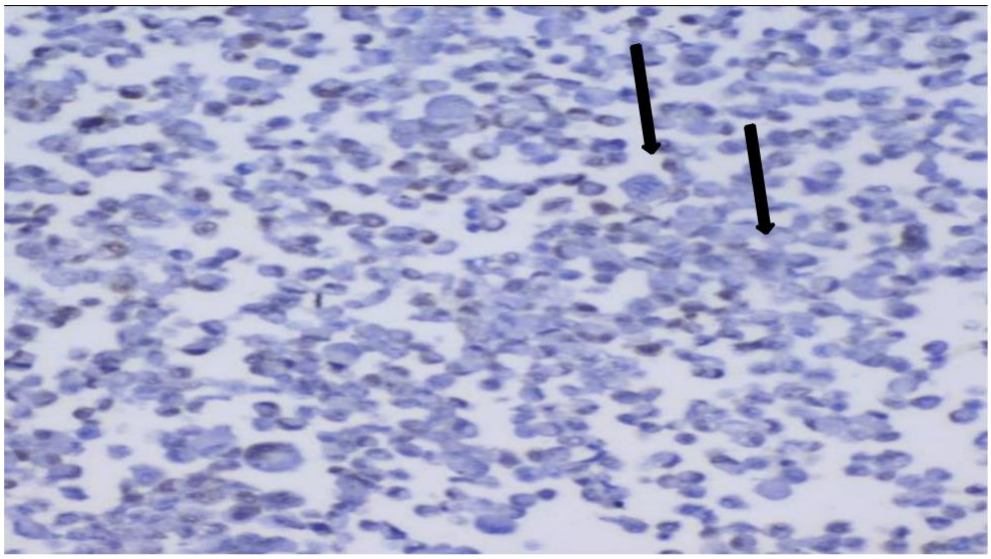

Fig. (18): A Photomicrograph of EXR/C2 group shows weak nuclear Slug immune expression (Black arrows) (ABC x 100).

Journal of Chemical Health Risks

www.jchr.org

JCHR (2024) 14(1), 629-646 | ISSN:2251-6727

Mean and SD values of area percentage of all groups were presented in table (4) and Fig. (19) which show a highly significant difference between groups with P ≤ 0.001. In a multiple comparison Tukey's test, there was a highly significantly different values between all groups except between EXR group and EXC2 group which revealed a significant difference with p-value = 0.038. On the other hand, no significant different was between EXC5 and EXR/C2 groups, which revealed P-value = 0.099 (P > 0.05) as shown in table (4).

Table (4): Mean and SD of area percent of slug immunoexpression in control and experimental groups (One-way ANOVA - test).

Area percent% expressions of Slug marker				
Groups	Mean (%) ± SD	Min—Max	F	P-value
A	41.25±0.96	40.31—42.23	199.676	0.001**
EXR	28.36±2.11	26.23—30.43		
EXC2	23.87±1.07	22.65—24.68		
EXC5	12.52±1.72	10.79—14.22		
EXR/C2	8.82±1.79	6.99—10.59		

**P ≤ 0.001 is highly significant

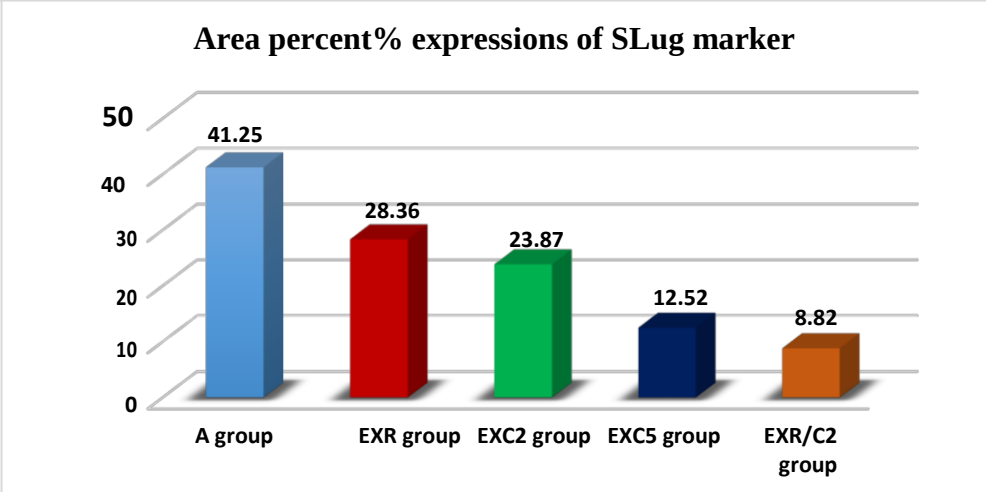

Fig. (19): Bar chart diagram showing area percent expression of slug marker of cancer cells in all groups.

Table (5): Difference between area percent of the studied groups measured by Tukey's test.

Multiple comparison Tukey's test of area percent% expressions of Slug marker					
Groups	A	EXR	EXC2	EXC5	EXR/C2
A	------	0.001**	0.001**	0.001**	0.001**
EXR	0.001**	------	0.038*	0.001**	0.001**
EXC2	0.001**	0.038*	------	0.001**	0.001**
EXC5	0.001**	0.001**	0.001**	------	0.099
EXR/C2	0.001**	0.001**	0.001**	0.099	------

P> 0.5 is not significant, *P ≤ 0.05 is significant while **P ≤ 0.001 is highly significant.

Journal of Chemical Health Risks

www.jchr.org

JCHR (2024) 14(1), 629-646 | ISSN:2251-6727

4. Discussion

Oral squamous cell carcinoma (OSCC) is considered as an invasive and aggressive malignancy with the potential to promote early metastasis and extensive lymph node involvement, therefore, it has a poor prognosis [19]. Despite significant improvements in OSCC treatment, a high mortality rate still exists. To date, chemotherapy remains the standard therapy for cancer treatments. Unfortunately, the significant toxicity of clinically implemented anticancer agents to normal tissues represents an unavoidable barrier for cancer treatment. In order to minimize the damaging consequences of chemotherapy, much researches have focused on the use of herbal medicine in cancer treatment protocols [20]. One of the primaries aims in the creation of auxiliary chemotherapy medications was to increase the sensitivity of cancerous cells to chemotherapeutic agents. Fortunately, recent investigations have shown that RSV increases this sensitivity. Despite its beneficial biological functions, RSV is a natural compound and has certain limitations in curing multiple diseases when used as monotherapy, especially for cancer [21]. In a trial to overcome the problems associated with the high dose of Cis, the effects of RSV alone or in combination with different doses of Cis on the viability, migration and epithelial mesenchymal transition (EMT) of tongue squamous cell carcinoma (TSCC) were investigated in the present study.

The results of the present study showed a significant decrease in cell viability of CAL-27 cell lines in EXR group compared to the control group. RSV exhibited cytotoxicity in a dose dependent manner. It denotes the response of TSCC to the inhibitory effects of RSV. This finding coincides with Park et al., (2020) who found that RSV inhibited the proliferation of OSCC (YD-10B) cells that were dose dependent [22]. In the same line, Silk et al., (2021) documented that RSV inhibited the proliferation of prostate cancer cell lines through targeting the tumor microenvironment, which plays important roles in the initiation of tumors [23] .

Xiao et al., (2021) explained that RSV inhibits malignant proliferation of CAL-27 cell lines via apoptotic pathway by activation of the zinc finger protein 750 signaling pathway and modification of the tumor vascular microenvironment [24]. In addition, this finding is agreement with Chen et al., (2020) who found that OSCC (HSC-3) were sensitive to RSV and exhibit inhibition of proliferation meanwhile promoting apoptosis through the inhibition of chromobox protein homolog 7 (CBX7), it was demonstrated that CBX7 was increased in OSCC, and it had a closely association with worse overall survival through the activation of Akt pathway [25] .

Many other studies have demonstrated that RSV has the ability to initiate cell death in pancreatic[26], prostatic[27], and hepatic cancer cells [28]. In contrast, Castillo-Pichardo et al., (2013) found that RSV accelerated the proliferation and metastasis of xenografted mouse breast cancers [29]. It is suggested that further research is necessary. This controversy is attributed to the differences in methodology and doses as they used immunocompromised mice and employed a small amount of RSV.

The IC50 of RSV in the current study was 28.45 µg/ml, while Dong et al., (2016) reported that the IC50 was 1 µg/ml, for OSCC (SCC-25) cell lines [30]. They used Aqueous One Solution Cell Proliferation (MTS) assay and different types of cell lines.

The proliferation inhibition of CAL-27 after application of Cis was evaluated. The results of the present study showed that Cis had a concentration dependent antiproliferative effect against TSCC. These findings support the results of Chen et al., (2017) who showed that Cis reduced OSCC CAL-27 growth, and the rate of inhibition was dependent on the drug dose [31]. Also, Bijani et al., (2021). reported that the cytotoxic effect of Cis has been enhanced with increasing the drug concentration on OSCC cell line HN5 [20]. This finding represented the sensitivity of cultured malignant cells to the suppression effects of Cis. It was obvious in the results of Alonso et al., (2020) who demonstrated that as the dose of Cis increased, OSCC H357 cell viability decreased [32]. In the current work, IC50 of Cis was 1.93 µg/ml which is nearly the same IC50 of Helal et al., (2015) who reported that the IC50 was 1.3 µg/ml on TSCC [32].

In this study, simultaneous application of RSV and Cis to cultured carcinoma cells resulted in a significant decrease of viable cells compared to control group or to groups treated with RSV and Cis alone. This denotes that RSV exerted anticancer effects and enhanced the proliferation inhibitory effect of Cis on TSCC CAL-27 cell lines.

It is noteworthy that the application of RSV with a low dose of Cis (2 µg/ml) exhibited a greater inhibition

Journal of Chemical Health Risks

www.jchr.org

JCHR (2024) 14(1), 629-646 | ISSN:2251-6727

effect than a high dose of Cis (5 µg/ml) alone on the viability of cancer cells. The mean of viability was 15% for EXR/C2 group while it was 19% for EXC5, with a highly significant difference ($P \leq 0.001$).

This finding is in agreement with Li Ma et al., (2015) who reported that RSV revealed anticancer effects on non-small cell lung cancer H838 and H520 cell lines. They explained that RSV enhanced the antitumor effects of Cis through inducing mitochondrial apoptotic pathway by depolarization of mitochondrial membrane potential, release of cytochrome c, and increased expression of proapoptotic (Bcl-2 and Bax) proteins [9].

In addition, the current results are also in the same line with Galicia et al., (2018) who reported that RSV significantly enhanced the anti-proliferative effects of Cis in both breast cancer cell lines (MCF-7 and MCF-7R) [33]. These studies suggested that RSV increases the sensitivity of cancer cell lines to Cis.

In the current study, the influence of RSV and Cis alone or in combination on morphology of CAL-27 cell lines compared to control group was examined by inverted phase contrast microscopy. The cells of experimental groups were sparse with decreased cell number and loss of cell attachment. Single cells displayed many morphological alterations as changed from polygonal shape to rounded outline. Scattered individual cells exhibited apoptosis revealed by condensed chromatin with blebbing of cell membrane. These changes increased in combined (EXR/C2 and EXR/C5) groups, compared to the changes observed in single-agent treatment (EXR, EXC2 &EXC5). These findings suggested that combinations of RSV with Cis decrease cell number and induce apoptosis in TSCC cell line more than RSV or Cis alone treatments. This is in agreement with Ren et al., (2020) who showed that RSV enhanced the effects of Cis on the alteration of morphology of gastric cancer (AGS cell lines) [33].

By using a wound healing assay, the effects of RSV and Cis on the migration of CAL-27 cells through 48 hours have been assessed. The results revealed that the wound healing width ratio of EXR group was 54.8% of the original width (0.9 mm) while it was 93.3% for the control group. This result suggested that RSV inhibited the migration of cancer cells. This outcome is in the same line with Kim et al., (2012) who studied the effects of RSV on the migration of OSCC [34]. Several studies reported that RSV has antimigratory effect on other different cancers cell lines such as breast-cancer cells [35], metastatic lung and cervical cancer cells [36], ovarian cancer[37] and OSCC [38].

On the contrary, these results are not matched with Gweon and Kim (2013) who informed that RSV increases the cell migratory ability of HT1080 human fibrosarcoma cells by inducing the activation and expression of MMP 9 [39]. The wound gap was wider in the Cis groups (EXC2 and EXC5) compared to RSV group (EXR), as the width closure was 45.7%, 32.4% and 54.8%, respectively, with ($P \leq 0.001$).

In addition, the results showed that RSV combined with Cis synergistically inhibited cell migration. A highly statistically significant inhibition in the migration of CAL-27 cells in combined groups (EXR/C2 and EXR/C5) was noted compared to control group as well as separate treated groups (EXR, EXC2 and EXC5) with ($P \leq 0.001$). Specifically, the antimigratory effect of EXR/C2 was more than that of EXC5, the width closure was 22.6% and 32.4%, respectively with ($P \leq 0.001$).

These results indicated that RSV sensitizes the inhibitory effects of Cis on migration of CAL-27 cells. These results consistent with Yang et al., (2021) who reported that RSV combined with Cis inhibited cell migration of breast cancer cell lines MDA231 through inhibition of TGFβ1-induced cell migration and invasion [40]. Regardless to Cis, these findings are in the same line with Chung et al., (2018(who suggested that combined RSV and 5-flurouracil enhanced the inhibitory effects on the migration of human colorectal cancer cells [41] .

The EMT is a crucial cellular process that is important for the morphogenesis and homeostasis of solid tissues. In the earliest phase of cancer spread and invasion, cells lose their epithelial properties. ZEB1, Slug, and Snail are transcription factors that initiate EMT and stimulate invasion and metastasis of cancer cells. Because of its capability to bind to the promoter E-box, which inhibits the transcription of E-cadherin, Slug plays a crucial role in EMT [42] . In our study, EMT assessment by ICC expression of Slug in different groups was explored. Slug showed high activity among control group, while the expression levels of Slug were decreased in EXR group in comparison to control group. The significant difference between control and EXR groups was high statistically significant with ($P \leq 0.001$). This finding is in agreement with the work

Journal of Chemical Health Risks

www.jchr.org

JCHR (2024) 14(1), 629-646 | ISSN:2251-6727

conducted by Kim et al., (2018) on OSCC. They noticed that applying RSV inhibits EMT revealed by reduction of Slug expression [34].

The outcomes of our study matched those of Gao et al., (2015) who investigated Slug expression on gastric cancer cell lines. They showed that RSV-treated cells had lower levels of Slug than the control group. They indicated that RSV would be able to inhibit EMT and suppress invasion and metastasis in gastric cancer in vitro [43].

The effect of Cis on EMT showed decrease in the immunostaining of Slug in EXC2 & EXC5 groups in comparison to control group. The significant differences were statistically high ($P \leq 0.001$). These findings are in the same line with Wang et al., (2021) who analyzed malignant behavior of breast cancer upon applying Cis. They demonstrated that Cis inhibits cancer metastasis through blocking EMT[44]. Controversially, Wang et al., (2018) reported that Cis promotes tumor invasion and metastasis in a human lung cancer xenograft model through stimulation of tumor microenvironmental factors that are released from apoptotic cancer cells, facilitating the metastasis of neighboring cancer cells, and resulting in tumor progression [45].

In our study, unfortunately, because of the significant toxicity of combined RSV and high dose of Cis (EXR/C5), it was unable to produce a pellet for such group. In this study, interestingly, in EXR/C2 group the expression of Slug was more reduced compared to that in single agent treated groups (EXR and EXC2) as well as control group, with a high statistically significant difference ($P \leq 0.001$). These results indicated that RSV has adverse efficacy on EMT, and these effects were increased with Cis. This finding is supported by Yang et al., (2021) who studied the effects of RSV and Cis on EMT in breast cancer. They revealed that the expressions of E-cadherin significantly increased, while the expressions of mesenchymal markers decreased[40].

The idea of combination treatment with Cis and RSV is to minimize the dose of Cis and its compensation with RSV in order to minimize Cis side effect. The results of the current study revealed that RSV could potentiate the anticancer effect of low dose Cis on cancer cells and could decrease its toxicity. This is in agreement with REN et al., (2020) who concluded that RSV increased the beneficial effects of Cis and decreased its side effects against gastric cancer cells by inducing endoplasmic reticulum stress-mediated apoptosis and G2/M phase arrest [46].

Due to its anticancer efficiency, Cis usage as a chemotherapeutic drug is essential despite its side effects. From this point, Cis and RSV may be combined to maximize the benefits of chemotherapeutic agents while limiting the problems of Cis side effects.

5. Conclusion and recommendations

In conclusion, the synergistic application of RSV in conjunction with Cis emerges as a promising therapeutic strategy for oral squamous cell carcinoma (OSCC). This combined treatment has demonstrated notable efficacy in diminishing cancer cell viability, impeding migration, and restraining epithelial-mesenchymal transition (EMT) processes. The observed outcomes suggest a potentiation of therapeutic effects, showcasing the complementary actions of RSV and Cis in targeting OSCC. Importantly, the implementation of this dual approach has exhibited a favorable safety profile, minimizing undesirable side effects. Looking towards the future, the exploration of RSV and Cis combination therapy warrants further investigation and refinement. Subsequent research endeavors should delve into elucidating the underlying molecular mechanisms responsible for the observed synergies, paving the way for targeted interventions. Additionally, clinical studies are imperative to validate the translational potential of this approach, ensuring its efficacy and safety in human subjects. The continued exploration of this promising combination holds the potential to redefine the landscape of OSCC therapy, offering a more robust and targeted treatment modality that could significantly enhance patient outcomes. As we move forward, a deeper understanding of the molecular intricacies and clinical applicability of RSV and Cis combination therapy will undoubtedly contribute to its evolution as a forefront strategy in the battle against oral squamous cell carcinoma.

References

(1) Muzaffar, J.; Bari, S.; Kirtane, K.; Chung, C. H. Recent Advances and Future Directions in Clinical Management of Head and Neck Squamous Cell Carcinoma. *Cancers (Basel).* **2021**, *13* (2), 1–16. https://doi.org/10.3390/cancers13020338.

(2) Xie, L.; Shang, Z. Burden of Oral Cancer in

Asia from 1990 to 2019: Estimates from the Global Burden of Disease 2019 Study. *PLoS One* **2022**, *17* (3 March). https://doi.org/10.1371/journal.pone.0265950.

(3) Hernández-Morales, A.; González-López, B. S.; Scougall-Vilchis, R. J.; Bermeo-Escalona, J. R.; Velázquez-Enríquez, U.; Islas-Zarazúa, R.; Márquez-Rodríguez, S.; Sosa-Velasco, T. A.; Medina-Solís, C. E.; Maupomé, G. Lip and Oral Cavity Cancer Incidence and Mortality Rates Associated with Smoking and Chewing Tobacco Use and the Human Development Index in 172 Countries Worldwide: An Ecological Study 2019-2020. *Healthc. (Basel, Switzerland)* **2023**, *11* (8). https://doi.org/10.3390/healthcare11081063.

(4) Freier, K.; Hofele, C.; Knoepfle, K.; Gross, M.; Devens, F.; Dyckhoff, G.; Plinkert, P.; Lichter, P.; Herold-Mende, C. Cytogenetic Characterization of Head and Neck Squamous Cell Carcinoma Cell Lines as Model Systems for the Functional Analyses of Tumor-Associated Genes. *J. Oral Pathol. Med.* **2010**, *39* (5), 382–389. https://doi.org/10.1111/j.1600-0714.2009.00864.x.

(5) Cheng, Y.; Li, S.; Gao, L.; Zhi, K.; Ren, W. The Molecular Basis and Therapeutic Aspects of Cisplatin Resistance in Oral Squamous Cell Carcinoma. *Front. Oncol.* **2021**, *11* (October), 1–16. https://doi.org/10.3389/fonc.2021.761379.

(6) de Lucas, B.; Pérez, L. M.; Gálvez, B. G. Importance and Regulation of Adult Stem Cell Migration. *J. Cell. Mol. Med.* **2018**, *22* (2), 746–754. https://doi.org/10.1111/jcmm.13422.

(7) Luo, H.; Guo, J.; Yu, B.; Chen, W.; Zhang, H.; Zhou, X.; Chen, Y.; Huang, L.; Liu, N.; Ren, X.; Yan, L.; Huai, D.; Lei, Y.; Liao, B.; Jiang, H. Construction of DdRADseq-Based High-Density Genetic Map and Identification of Quantitative Trait Loci for Trans-Resveratrol Content in Peanut Seeds. *Front. Plant Sci.* **2021**, *12*, 644402. https://doi.org/10.3389/fpls.2021.644402.

(8) Berretta, M.; Bignucolo, A.; Di Francia, R.; Comello, F.; Facchini, G.; Ceccarelli, M.; Iaffaioli, R. V.; Quagliariello, V.; Maurea, N. Resveratrol in Cancer Patients: From Bench to Bedside. *Int. J. Mol. Sci.* **2020**, *21* (8). https://doi.org/10.3390/ijms21082945.

(9) Ma, L.; Zhang, M.; Zhao, R.; Wang, D.; Ma, Y.; Li, A. Plant Natural Products: Promising Resources for Cancer Chemoprevention. *Molecules* **2021**, *26* (4). https://doi.org/10.3390/molecules26040933.

(10) Debela, D. T.; Muzazu, S. G.; Heraro, K. D.; Ndalama, M. T.; Mesele, B. W.; Haile, D. C.; Kitui, S. K.; Manyazewal, T. New Approaches and Procedures for Cancer Treatment: Current Perspectives. *SAGE open Med.* **2021**, *9*, 20503121211034370. https://doi.org/10.1177/20503121211034366.

(11) Singh, V.; Singh, R.; Kujur, P. K.; Singh, R. P. Combination of Resveratrol and Quercetin Causes Cell Growth Inhibition, DNA Damage, Cell Cycle Arrest, and Apoptosis in Oral Cancer Cells. *Assay Drug Dev. Technol.* **2020**, *18* (5), 226–238. https://doi.org/10.1089/adt.2020.972.

(12) Ma, L.; Li, W.; Wang, R.; Nan, Y.; Wang, Q.; Liu, W.; Jin, F. Resveratrol Enhanced Anticancer Effects of Cisplatin on Non-Small Cell Lung Cancer Cell Lines by Inducing Mitochondrial Dysfunction and Cell Apoptosis. *Int J Oncol* **2015**, *47* (4), 1460–1468. https://doi.org/10.3892/ijo.2015.3124.

(13) Chen, Y.; Hao, L.-J.; Hung, C.; Chen, J.; Leu, S.; Huang, B. Apoptotic Effect of Cisplatin and Cordycepin on OC3 Human Oral Cancer Cells. *Chin. J. Integr. Med.* **2014**, *20* (8), 624–632. https://doi.org/10.1007/s11655-013-1453-3.

(14) Uchikado, Y.; Natsugoe, S.; Okumura, H.; Setoyama, T.; Matsumoto, M.; Ishigami, S.; Aikou, T. Slug Expression in the E-Cadherin Preserved Tumors Is Related to Prognosis in Patients with Esophageal Squamous Cell Carcinoma. *Clin. cancer Res. an Off. J. Am. Assoc. Cancer Res.* **2005**, *11* (3), 1174–1180.

(15) Xu, J.; Liu, D.; Niu, H.; Zhu, G.; Xu, Y.; Ye, D.; Li, J.; Zhang, Q. Resveratrol Reverses DoxorubicinResistancebyInhibiting Epithelial-Mesenchymal Transition (EMT) through Modulating PTEN/Akt Signaling Pathway in Gastric Cancer. *J. Exp. Clin. Cancer Res.* **2017**, *36* (1), 19. https://doi.org/10.1186/s13046-016-0487-8.

(16) Mota, A. de L.; Evangelista, A. F.; Macedo, T.; Oliveira, R.; Scapulatempo-Neto, C.; Vieira, R. A.; Marques, M. M. C. Molecular

Characterization of Breast Cancer Cell Lines by Clinical Immunohistochemical Markers. *Oncol. Lett.* **2017**, *13* (6), 4708–4712. https://doi.org/10.3892/ol.2017.6093.

(17) Lozon, L.; Saleh, E.; Menon, V.; Ramadan, W. S.; Amin, A.; El-Awady, R. Effect of Safranal on the Response of Cancer Cells to Topoisomerase I Inhibitors: Does Sequence Matter? *Front. Pharmacol.* **2022**, *13*, 938471. https://doi.org/10.3389/fphar.2022.938471.

(18) Ramos-Vara, J. A. Technical Aspects of Immunohistochemistry. *Vet. Pathol.* **2005**, *42* (4), 405–426. https://doi.org/10.1354/vp.42-4-405.

(19) Bugshan, A.; Farooq, I. Oral Squamous Cell Carcinoma: Metastasis, Potentially Associated Malignant Disorders, Etiology and Recent Advancements in Diagnosis. *F1000Research* **2020**, *9*, 229. https://doi.org/10.12688/f1000research.22941.1.

(20) Bijani, F.; Zabihi, E.; Bijani, A.; Nouri, H. R.; Nafarzadeh, S.; Seyedmajidi, M. Evaluation of Apoptotic Effect of Crocin, Cisplatin, and Their Combination in Human Oral Squamous Cell Carcinoma Cell Line HN5. *Dent. Res. J. (Isfahan).* **2021**, *18*, 70.

(21) Chang, W.-S.; Tsai, C.-W.; Yang, J.-S.; Hsu, Y.-M.; Shih, L.-C.; Chiu, H.-Y.; Bau, D.-T.; Tsai, F.-J. Resveratrol Inhibited the Metastatic Behaviors of Cisplatin-Resistant Human Oral Cancer Cells via Phosphorylation of ERK/p-38 and Suppression of MMP-2/9. *J. Food Biochem.* **2021**, *45* (6), e13666. https://doi.org/10.1111/jfbc.13666.

(22) PARK, K.-E.; OK, C.-Y.; JANG, H.-O.; BAE, M.-K.; BAE, S.-K. Resveratrol Inhibits Cell Growth via Targeting the Bmi-1 Pathway in YD-10B Human Oral Squamous Cell Carcinoma Cells. *Int. J. Oral Biol.* **2020**, *45* (3), 115–125.

(23) Silk, N.; Reich, J.; Sinha, R.; Chawla, S.; Geary, K.; Zhang, D. The Effects of Resveratrol on Prostate Cancer through Targeting the Tumor Microenvironment. *J. xenobiotics* **2021**, *11* (1), 16–32. https://doi.org/10.3390/jox11010002.

(24) Xiao, Y.; Duan, Y.; Wang, Y.; Yin, X. Resveratrol Suppresses Malignant Progression of Oral Squamous Cell Carcinoma Cells by Inducing the ZNF750/RAC1 Signaling Pathway. *Bioengineered* **2021**, *12* (1), 2863–2873. https://doi.org/10.1080/21655979.2021.1940616.

(25) Chen, L.; Xia, J.-S.; Wu, J.-H.; Chen, Y.-G.; Qiu, C.-J. Resveratrol Inhibits Oral Squamous Cell Carcinoma Cells Proliferation While Promoting Apoptosis through Inhibition of CBX7 Protein. *Environ. Toxicol.* **2020**, *35* (11), 1234–1240. https://doi.org/10.1002/tox.22988.

(26) Jiang, Z.; Chen, X.; Chen, K.; Sun, L.; Gao, L.; Zhou, C.; Lei, M.; Duan, W.; Wang, Z.; Ma, Q.; Ma, J. YAP Inhibition by Resveratrol via Activation of AMPK Enhances the Sensitivity of Pancreatic Cancer Cells to Gemcitabine. *Nutrients* **2016**, *8* (10). https://doi.org/10.3390/nu8100546.

(27) Sheth, S.; Jajoo, S.; Kaur, T.; Mukherjea, D.; Sheehan, K.; Rybak, L. P.; Ramkumar, V. Resveratrol Reduces Prostate Cancer Growth and Metastasis by Inhibiting the Akt/MicroRNA-21 Pathway. *PLoS One* **2012**, *7* (12), e51655. https://doi.org/10.1371/journal.pone.0051655.

(28) Rahman, M.; Almalki, W. H.; Afzal, O.; Altamimi, A. S. A.; Kazmi, I.; Al-Abbasi, F. A.; Choudhry, H.; Alenezi, S. K.; Barkat, M. A.; Beg, S.; Kumar, V.; Alhalmi, A. Cationic Solid Lipid Nanoparticles of Resveratrol for HepatocellularCarcinomaTreatment: Systematic Optimization, in Vitro Characterization and Preclinical Investigation. *Int. J. Nanomedicine* **2020**, *15*, 9283–9299. https://doi.org/10.2147/IJN.S277545.

(29) Castillo-Pichardo, L.; Cubano, L. A.; Dharmawardhane, S. Dietary Grape Polyphenol Resveratrol Increases Mammary Tumor Growth and Metastasis in Immunocompromised Mice. *BMC Complement. Altern. Med.* **2013**, *13*, 6. https://doi.org/10.1186/1472-6882-13-6.

(30) Yu, X.-D.; Yang, J.-L.; Zhang, W.-L.; Liu, D.-X. Resveratrol Inhibits Oral Squamous Cell Carcinoma through Induction of Apoptosis and G2/M Phase Cell Cycle Arrest. *Tumour Biol. J. Int. Soc. Oncodevelopmental Biol. Med.* **2016**, *37* (3), 2871–2877. https://doi.org/10.1007/s13277-015-3793-4.

(31) Chen, S.; Hu, H.; Miao, S.; Zheng, J.; Xie, Z.; Zhao, H. Anti-Tumor Effect of Cisplatin in Human Oral Squamous Cell Carcinoma Was Enhanced by Andrographolide via Upregulation of Phospho-P53 in Vitro and in Vivo. *Tumour Biol. J. Int. Soc. Oncodevelopmental Biol. Med.* **2017**, *39* (5), 1010428317705330. https://doi.org/10.1177/1010428317705330.

(32) Camacho-Alonso, F.; Gómez-Albentosa, T.; Oñate-Sánchez, R. E.; Tudela-Mulero, M. R.; Sánchez-Siles, M.; Gómez-García, F. J.; Guerrero-Sánchez, Y. In Vitro Study of Synergic Effect of Cisplatin and Low Molecular Weight Heparin on Oral Squamous Cell Carcinoma. *Front. Oncol.* **2020**, *10*, 549412. https://doi.org/10.3389/fonc.2020.549412.

(33) Leon-Galicia, I.; Diaz-Chavez, J.; Albino-Sanchez, M. E.; Garcia-Villa, E.; Bermudez-Cruz, R.; Garcia-Mena, J.; Herrera, L. A.; García-Carrancá, A.; Gariglio, P. Resveratrol Decreases Rad51 Expression and Sensitizes Cisplatin-resistant MCF-7 Breast Cancer Cells. *Oncol. Rep.* **2018**, *39* (6), 3025−3033. https://doi.org/10.3892/or.2018.6336.

(34) Kim, S.-E.; Shin, S.-H.; Lee, J.-Y.; Kim, C.-H.; Chung, I.-K.; Kang, H.-M.; Park, H.-R.; Park, B.-S.; Kim, I.-R. Resveratrol Induces Mitochondrial Apoptosis and Inhibits Epithelial-Mesenchymal Transition in Oral Squamous Cell Carcinoma Cells. *Nutr. Cancer* **2018**, *70* (1), 125−135. https://doi.org/10.1080/01635581.2018.1397708.

(35) Tang, F.-Y.; Su, Y.-C.; Chen, N.-C.; Hsieh, H.-S.; Chen, K.-S. Resveratrol Inhibits Migration and Invasion of Human Breast-Cancer Cells. *Mol. Nutr. Food Res.* **2008**, *52* (6), 683−691. https://doi.org/10.1002/mnfr.200700325.

(36) Kim, Y. S.; Sull, J. W.; Sung, H. J. Suppressing Effect of Resveratrol on the Migration and Invasion of Human Metastatic Lung and Cervical Cancer Cells. *Mol. Biol. Rep.* **2012**, *39* (9), 8709−8716. https://doi.org/10.1007/s11033-012-1728-3.

(37) Ferraresi, A.; Phadngam, S.; Morani, F.; Galetto, A.; Alabiso, O.; Chiorino, G.; Isidoro, C. Resveratrol Inhibits IL-6-Induced Ovarian Cancer Cell Migration through Epigenetic up-Regulation of Autophagy. *Mol. Carcinog.* **2017**, *56* (3), 1164−1181. https://doi.org/10.1002/mc.22582.

(38) Shan, Z.; Yang, G.; Xiang, W.; Pei-jun, W.; Bin, Z. Effects of Resveratrol on Oral Squamous Cell Carcinoma (OSCC) Cells in Vitro. *J. Cancer Res. Clin. Oncol.* **2014**, *140* (3), 371−374. https://doi.org/10.1007/s00432-013-1575-1.

(39) Gweon, E. J.; Kim, S. J. Resveratrol Induces MMP-9 and Cell Migration via the P38 Kinase and PI-3K Pathways in HT1080 Human Fibrosarcoma Cells. *Oncol. Rep.* **2013**, *29* (2), 826−834. https://doi.org/10.3892/or.2012.2151.

(40) Yang, M.-D.; Sun, Y.; Zhou, W.-J.; Xie, X.-Z.; Zhou, Q.-M.; Lu, Y.-Y.; Su, S.-B. Resveratrol Enhances Inhibition Effects of Cisplatin on Cell Migration and Invasion and Tumor Growth in Breast Cancer MDA-MB-231 Cell Models In Vivo and In Vitro. *Molecules* **2021**, *26* (8). https://doi.org/10.3390/molecules26082204.

(41) Chung, S. S.; Dutta, P.; Austin, D.; Wang, P.; Awad, A.; Vadgama, J. V. Combination of Resveratrol and 5-Flurouracil Enhanced Anti-Telomerase Activity and Apoptosis by Inhibiting STAT3 and Akt Signaling Pathways in Human Colorectal Cancer Cells. *Oncotarget* **2018**, *9* (68), 32943−32957. https://doi.org/10.18632/oncotarget.25993.

(42) Chen, K.-Y.; Chen, C.-C.; Chang, Y.-C.; Chang, M.-C.ResveratrolInducedPremature Senescence and Inhibited Epithelial-Mesenchymal Transition of Cancer Cells via Induction of Tumor Suppressor Rad9. *PLoS One* **2019**, *14* (7), e0219317. https://doi.org/10.1371/journal.pone.0219317.

(43) Al-Hamaideh, K. D.; Dmour, I.; El-Elimat, T.; Afifi, F. U. Uplc-Ms Profile and Anti-Proliferative Activity of the Berries of an Aggressive Wild-Growing Weed: Solanum Elaeagnifolium Cav. (Solanaceae). *Trop. J. Nat. Prod. Res.* **2020**, *4* (12), 1131−1138. https://doi.org/10.26538/tjnpr/v4i12.16.

(44) Wang, H.; Guo, S.; Kim, S.-J.; Shao, F.; Ho, J. W. K.; Wong, K. U.; Miao, Z.; Hao, D.; Zhao, M.; Xu, J.; Zeng, J.; Wong, K. H.; Di, L.; Wong, A. H.-H.; Xu, X.; Deng, C.-X. Cisplatin Prevents Breast Cancer Metastasis through Blocking Early EMT and Retards Cancer Growth Together with Paclitaxel. *Theranostics*

2021, *11* (5), 2442−2459. https://doi.org/10.7150/thno.46460.

(45) Wang, K.; Shan, S.; Wang, S.; Gu, X.; Zhou, X.; Ren, T. HMGB1-Containing Nucleosome Mediates Chemotherapy-Induced Metastasis of Human Lung Cancer. *Biochem. Biophys. Res. Commun.* **2018**, *500* (3), 758−764. https://doi.org/10.1016/j.bbrc.2018.04.150.

(46) Ren, M.; Zhou, X.; Gu, M.; Jiao, W.; Yu, M.; Wang, Y.; Liu, S.; Yang, J.; Ji, F. Resveratrol Synergizes with Cisplatin in Antineoplastic Effects against AGS Gastric Cancer Cells by InducingEndoplasmicReticulum Stress-mediated Apoptosis and G2/M Phase Arrest. *Oncol. Rep.* **2020**, *44* (4), 1605−1615. https://doi.org/10.3892/or.2020.7708.